Low-Frequency Contact Noise of GaN Nanowire Device Detected by Cross-Spectrum Technique

2011 Jpn. J. Appl. Phys. 50 06GF21

(http://iopscience.iop.org/1347-4065/50/6S/06GF21)

Japanese Journal of Applied Physics **50** (2011) 06GF21 **REGULAR PAPER**
DOI: 10.1143/JJAP.50.06GF21

Low-Frequency Contact Noise of GaN Nanowire Device Detected by Cross-Spectrum Technique

Liang-Chen Li*, Kuo-Hsun Huang[1], Jia-An Wei[1], Yuen-Wuu Suen[1,2,3], Ting-Wei Liu[4], Chia-Chun Chen[4], Li-Chyong Chen[5], and Kuei-Hsien Chen[6]

Center for Nano Science and Technology, National Chiao Tung University, Hsinchu 300, Taiwan
[1]*Department of Physics, National Chung Hsing University, Taichung 402, Taiwan*
[2]*Institute of Nanoscience, National Chung Hsing University, Taichung 402, Taiwan*
[3]*National Nano Device Laboratories, Hsinchu 300, Taiwan*
[4]*Department of Chemistry, National Taiwan Normal University, Taipei 116, Taiwan*
[5]*Center for Condensed Matter Sciences, National Taiwan University, Taipei 106, Taiwan*
[6]*Institute of Atomic and Molecular Sciences, Academia Sinica, Taipei 106, Taiwan*

Received November 30, 2010; revised January 13, 2011; accepted January 29, 2011; published online June 20, 2011

We report the properties of low-frequency contact noise of multielectrode GaN nanowire (NW) devices. A two-port cross-spectrum technique is used to discriminate the noise of the ohmic contact from that of the NW section. The diameter of the GaN NW is around 100 nm. The Ti/Al electrodes of the NWs are defined by e-beam lithography. The typical resistance of a NW section with a length of 800 nm is about 5.5 kΩ and the two-wire resistance is below 100 kΩ. The results show that the low-frequency excess noise of the GaN NW is much smaller than that of the current-flowing contact, indicating that the contact noise dominates the noise behavior in our GaN NW devices. A careful study of the noise amplitude (A) of the $1/f$ noise of different types of NW and carbon nanotube devices, both in our work and in the literature, yields an empirical formula for estimating A from the two-wire resistance of the device.

1. Introduction

For decades, semiconductor nanowires (NWs) have become potential building blocks of nanometer-scale devices.[1)] Among them, GaN NWs have drawn much attention in terms of nanoelectronics and photonic devices. The field effect transistors (FETs) based on individual GaN NWs were shown to exhibit good switching behaviors with very large conductance swings controlled by the gates.[2)] Crossed NW p–n junctions assembled from p-type Si and n-type GaN NWs[2)] were also demonstrated to show a promising rectifying electrical property, and various logic gates were also successfully constructed therefrom.[3)] An internal p–n junction within a single GaN NW[4)] was fabricated by introducing a Mg doping source halfway into the NW synthesis process, and the temperature dependence of the rectification behavior down to 2.6 K was carefully studied. Tunable electroluminescence from 365 to 600 nm was demonstrated for core/multishell NW radial heterostructures with an n-type GaN core and InGaN/GaN/p-AlGaN/p-GaN shells,[5)] which can be used as multicolor light sources in integrated photonic systems.

The contacts connecting NWs to the outer world play an essential role in determining the performance of these nanoelectronic devices. The reduced dimensions of NWs and contacts make NW devices less immune to environmental fluctuations, such as redistribution of the impurity charges nearby, change in carrier number in the channel, and path switching of the carriers, and therefore may cause more excess noise than micrometer-scale devices. The excess noise in carbon nanotube (CNT) devices has been extensively studied.[6–12)] For example, Collins *et al.*[6)] and Ouacha *et al.*[7)] reported the strongly enhanced $1/f$ noise in single-wall and multiwall CNT devices compared with other conductor and semiconductor devices. Besides CNT devices, there are many works regarding the noise behavior of semiconductor NW devices in the literature. Xiong *et al.*[13)] demonstrated that the ZnO NW FET exhibits Lorentzian noise at 4.2 K, whereas only $1/f$ noise is observed at room temperature. Rumyantsev *et al.*[14)] reported $1/f$ noise in GaN NW transistors, and also found a generation–recombination noise near 1 kHz at high bias voltage. However, in most of the works mentioned above a two-wire noise measurement technique was used, which cannot distinguish the noise signals of the NW material from those of the contacts.

In this study, we use a cross-spectrum measurement to separate the excess noise spectrum of the ohmic contact of a GaN NW device from that of the NW section alone. Our results show that the low-frequency noise of the GaN NW device is dominated by the $1/f$ noise from the contact region through which a finite bias current flows. The Lorentzian noise may emerge from the $1/f$ background when the current is sufficiently high enough.

2. Experimental Procedure

N-type GaN NWs grown along the c-axis by the vapor-liquid-solid method[15,16)] were first dispersed in alcohol and then spread on a silicon substrate with a 3000 Å silicon dioxide layer. Several 300–400-nm-wide Al, Ti/Al, or Ti/Au electrodes connected to the NW were defined by the e-beam lithography technique, and then annealed at 400 °C. The diameter of GaN NW is around 100 nm. The typical two-wire resistance of the samples ranges from about 6 to 300 kΩ. The two-wire current–voltage (I–V) characteristics of each pair of contacts were carefully checked for linearity before noise measurements.

Figure 1(a) shows the SEM micrograph of a typical multielectrode GaN NW device, which, in part, can be modeled as a four-terminal NW device, as shown in schematically Fig. 1(b), and consists of three NW sections and four contact regions that connect the measurement system. Here, we first focus on the results for one of the samples with the bias current being applied between terminal 1 and terminal 4, as indicated by the blue dashed line. Figure 1(c) shows the equivalent circuit of a four-wire

*E-mail address: lcli@faculty.nctu.edu.tw

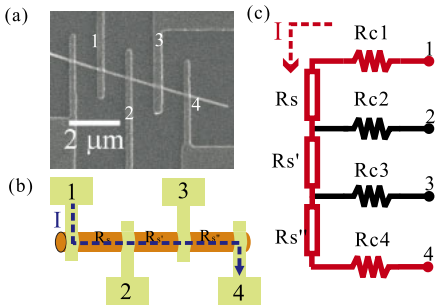

Fig. 1. (Color online) (a) SEM image, (b) schematics, and (c) equivalent circuit of a four-wire GaN nanowire device.

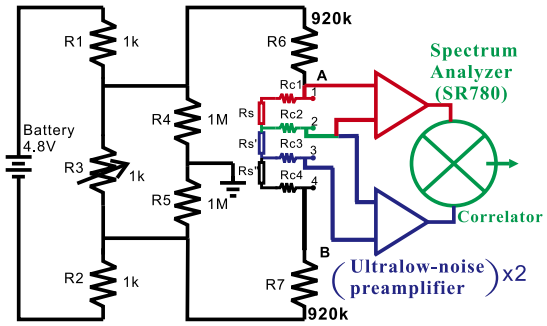

Fig. 2. (Color online) Schematic diagram of cross-spectrum measurement on a four-wire device. A balanced resistor network powered by a battery bank provides a DC bias current. This specific wiring is for measuring the correlation between ports 12 and 23.

NW device, which contains four resistors, Rc1, Rc2, Rc3, and Rc4, representing the ohmic contacts, and three resistors, Rs, Rs′, and Rs″, representing the NW sections separated by the electrodes. Their resistance values can be obtained directly by two-wire and four-wire I–V measurements.

Two configurations are used for noise characterization: a direct single-port measurement and a two-port correlation measurement. In the first configuration, voltage signals across two terminals, i.e., a single port, are fed into a set of low-noise preamplifiers and followed by a network signal analyzer, SR780 (Stanford Research Systems), which can calculate the fast Fourier transform (FFT) of the input signal and give the noise spectrum or the power spectral density (PSD). In the second configuration, voltage signals from two different ports are fed into two independent sets of low-noise preamplifiers and then read by two input channels of SR780, where their cross-spectrum[17] is calculated. Each preamplifier set consists of a home-made ultralow-noise JFET-input preamplifier followed by a commercial preamplifier, SR560 (Stanford Research Systems). If a long data acquisition time is required, a computer is used to record the data and perform the FFT or cross-spectrum calculations. To minimize the effect of pick-up noise, a balanced resistor network powered by a battery bank, as shown in Fig. 2, provides the bias current (I) for the sample.

The data from the single-port noise measurement usually give an inseparable spectrum that comprises the noise signals of contacts and the NW. For example, the PSD of the voltage across terminals 2 and 3 (i.e., port 23) in Fig. 2 can be written as

$$S_{23} = \langle V_{23}^2 \rangle = \langle (V_{\mathrm{Rc2}} + V_{\mathrm{Rs'}} + V_{\mathrm{Rc3}})^2 \rangle = \langle V_{\mathrm{Rc2}}^2 \rangle + \langle V_{\mathrm{Rs'}}^2 \rangle + \langle V_{\mathrm{Rc3}}^2 \rangle = S_{\mathrm{Rc2}} + S_{\mathrm{Rs'}} + S_{\mathrm{Rc3}}, \quad (1)$$

where the angle bracket denotes the spectral average and gives the PSD with the unit V^2/Hz. V_{Rc2}, $V_{\mathrm{Rs'}}$, and V_{Rc3} are the voltage noise signals generated by Rc2, Rs′, and Rc3, respectively. Here, the correlation terms between different contacts and NW sections are neglected. Clearly, with a single one-port noise measurement, we cannot separate S_{Rc2} or S_{Rc3} from $S_{\mathrm{Rs'}}$. On the other hand, a two-port correlation measurement can be used to extract the correlated part and eliminate the uncorrelated signals. Figure 2 illustrates a cross-spectrum measurement of ports 12 and 23, which yields the noise PSD of S_{Rc2}. The result can be represented as

$$\langle V_{12}^* \cdot V_{23} \rangle = \langle (V_{\mathrm{Rc1}} + V_{\mathrm{Rs}} + V_{\mathrm{Rc2}})^* \cdot (V_{\mathrm{Rc2}} + V_{\mathrm{Rs'}} + V_{\mathrm{Rc3}}) \rangle = \langle V_{\mathrm{Rc2}}^2 \rangle = S_{\mathrm{Rc2}}. \quad (2)$$

Similarly, the noise spectrum of the NW $S_{\mathrm{Rs'}}$ without the contact noise can be extracted via

$$\langle V_{14}^* \cdot V_{23} \rangle = \langle (V_{\mathrm{Rc1}} + V_{\mathrm{Rs}} + V_{\mathrm{Rs'}} + V_{\mathrm{Rs''}} + V_{\mathrm{Rc4}})^* \times (V_{\mathrm{Rc2}} + V_{\mathrm{Rs'}} + V_{\mathrm{Rc3}}) \rangle = \langle V_{\mathrm{Rs'}}^2 \rangle = S_{\mathrm{Rs'}}. \quad (3)$$

However, S_{Rc1} and S_{Rs} cannot be separated since there is no measurement terminal between Rc1 and Rs. Even so, we can still estimate their values if we assume that S_{Rs} and $S_{\mathrm{Rs'}}$ are almost the same in light of the same length of the NW sections they represent.

Before discussing the data, we comment on the issue regarding the correlation between different parts of the NW device. In fact, we have observed a very pronounced correlation effect in the frequency range where $1/f$ noise dominates from the cross-spectrum of the adjacent parts in some of the measurement configurations with current-flowing schemes different from this work.[18] The cross term, such as $\langle V_{\mathrm{Rs'}}^* \cdot V_{\mathrm{Rs}} \rangle$, sometimes indeed cannot be neglected in a nanometer-scale device. However, we have carefully checked the cross terms for the device presented in this work and found that they are very small and can be neglected. The underlying physics of the correlation effect is still unclear and further investigations are needed.

3. Results and Discussion

Normally, the PSD spectrum within the measurement bandwidth consists of a $1/f$ feature that is dominant at low frequencies (f) and flat white thermal noise at high frequencies. The thermal noise is directly related to the resistance of the component via $S_{\mathrm{Vthermal}} = 4kTR$ with k being Boltzmann's constant and T the temperature.[19,20] The GaN NW section between two adjacent electrodes has a length of 800 nm in the device presented in this work, and has a resistance (Rs or Rs′) of 5.5 kΩ. The contact resistance ranges from 2 to 19 kΩ. The resistance values derived from the thermal noise spectra are consistent with those obtained from direct two- or four-wire I–V measurements. We also note that the two-wire resistance of our samples is relatively low compared with the results in previous reports for GaN NW devices (from about 600 kΩ to more than MΩ).[2,14,15,21,22]

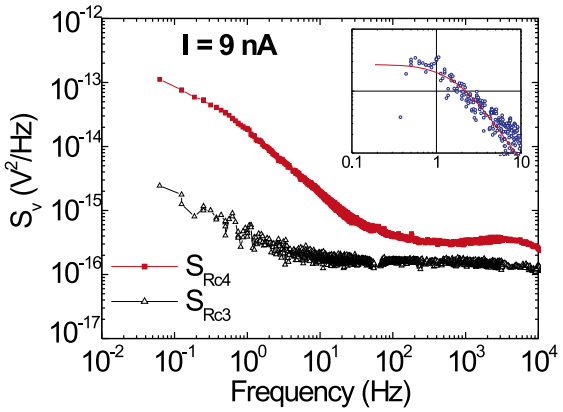

Fig. 3. (Color online) S_V spectrum of two different contacts, Rc4 and Rc3, at $I = 9$ nA. Rc4 is in the path of the bias current and shows more pronounced $1/f$ noise than does contact Rc3, which has no current. The inset shows the spectrum of S_{Rc4} after the $1/f$ noise and thermal noise have been subtracted, and the solid line shows the fitted result of a Lorentzian function.

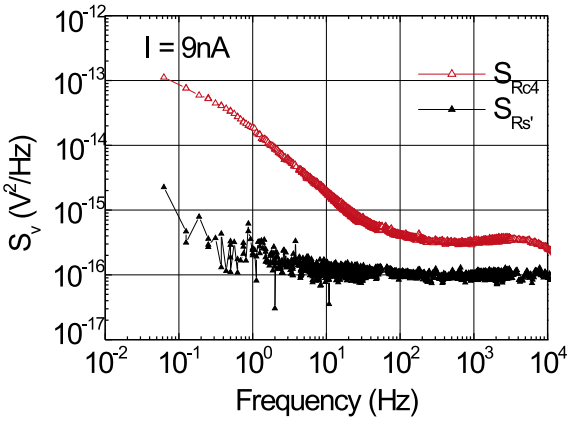

Fig. 4. (Color online) Noise spectra of contact Rc4 and a nanowire section Rs′ at $I = 9$ nA.

The noise spectrum of every individual component in the equivalent circuit shown in Fig. 1(c) can be extracted by using the correlation method described in the last section. Figure 3 shows the noise PSD of Rc3 and Rc4 as $I = 9$ nA running from terminal 1 to terminal 4. The corresponding resistances of Rc3 and Rc4 are 9 and 19 kΩ, respectively. Note that Rc4 is in the current-flowing path, whereas Rc3 is not. Apparently, the $1/f$ noise of Rc4 is much stronger than that of Rc3. As a matter of fact, the PSD of Rc3 does not change with I. Figure 4 shows S_{Rc4} and $S_{Rs'}$. Even though I goes through both Rs′ and Rc4, Rs′ does not exhibit clear $1/f$ noise as the contact does. At $f = 1$ Hz, the noise strength of Rc4 is almost two orders of magnitude higher than that of Rs′. We can summarize that the excess noise of the NW device in this study is dominated by the noise of the current-flowing contacts.

The inset of Fig. 3 shows the spectrum of Rc4 after the $1/f$ and thermal noise components have been subtracted. The data can be fitted with a Lorentzian function (solid line) with a characteristic frequency of 1.6 Hz. The burst noise waveform can also be observed in the captured time-domain data. This Lorentzian-like feature becomes more pronounced

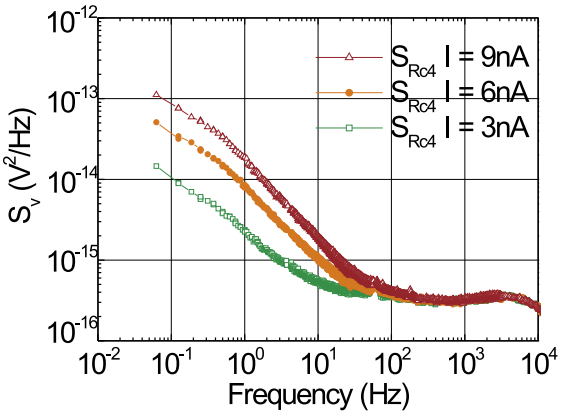

Fig. 5. (Color online) Noise spectra of contact Rc4 at different bias currents.

as I increases or T decreases. This can be attributed to the existence of a specific kind of traps with a fixed characteristic charging or discharging time.[23)]

Figure 5 shows the PSD of contact Rc4 at $I = 3$, 6, and 9 nA. The $1/f$ noise becomes more prominent as I increases. This behavior can be well described by a formula modified from Hooge's formula[24)] by Collins *et al.* for NW devices.[6)] The full spectrum can be expressed as the combination of $1/f$ noise and thermal noise:

$$S_V = A\frac{V^2}{f^\alpha} + S_{V\text{thermal}}, \tag{4}$$

where A is the noise amplitude and α a factor of order 1. Using a nonlinear fitting, we can obtain the value of A from the noise PSD spectrum. The value of A obtained here (two-port correlation measurements) is very close to that from the single-port data measured from terminals 4 and 3. This further confirms that the low-frequency excess noise property is determined by the current-flowing contact.

For carbon nanotubes, an empirical formula relating A and the two-wire resistance R has been reported:[6)] $A = 1 \times 10^{-11} R^{0.99}$; that is to say, A is roughly proportional to R. R is in the unit of Ω. Here, we collect two-wire (or single-port) noise data of more than ten GaN NW devices and three AlN NW devices,[25)] together with the data of CNT devices[6,9–12)] and ZnO NWs[13)] reported in the literature, and plot their values of A against R in a single figure, as shown in Fig. 6. A simple fitting yields $A = 3.6 \times 10^{-11} R^{0.98}$, which is very similar to the result reported by Collins *et al.*[6)] but with a larger proportional coefficient. The standard deviations in the prefactor are 3×10^{-12} and 0.18 in the power for R in the fitting. This formula provides an empirical guideline for estimating the order of magnitude of the noise amplitude of $1/f$ excess noise from the two-wire resistance R of NW devices, and is very useful in evaluating the device performance, especially in sensor-related applications.

Last but not the least, although the $1/f$ noise of ohmic contacts dominates the low-frequency excess noise in the NW devices in our study, which can only be categorized into low-resistance devices ($R < 100$ kΩ) in Fig. 6, it is not certain whether that the contact noise is also dominant in high-impedance NW devices, where the resistance of NWs

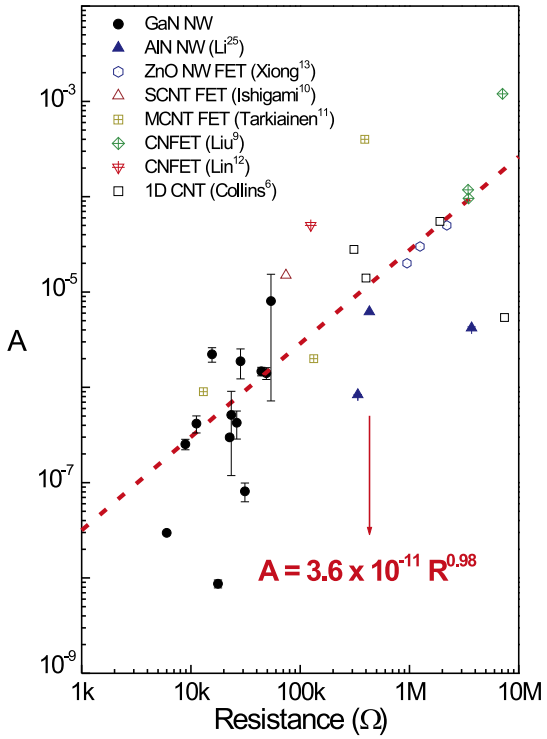

Fig. 6. (Color online) Noise amplitude (A) vs two-wire resistance (R) for different NW and CNT devices. The data of GaN and AlN NWs are from our work, and the others are from the reference listed at the end of each symbol legend.

may be much larger than the contact resistance. Further investigation is needed to clarify this issue.

4. Conclusions

We successfully determined the noise of individual contacts and NW sections of GaN NW devices by two-port cross-spectrum noise measurements. The result shows that the $1/f$ noise generated by the current-flowing ohmic contact dominates the low-frequency excess noise in multielectrode NW devices. Lorentzian noise is also observed embedded in the $1/f$ background at high bias currents. The $1/f$ noise generated by the semiconductor NW is much weaker than that of contacts even with a bias current. Thus, for our GaN NW devices with resistance below 100 kΩ, the contact noise is the major noise source in most two-wire devices. An empirical formula is also provided for estimating the noise amplitude of $1/f$ noise from the two-wire resistance of a NW device.

Acknowledgments

We acknowledge the support of the National Science Council of the Republic of China under Contract Nos. NSC-96-2112-M-005-004-MY3, NSC-99-2112-M-005-008, and NSC-99-2120-M-009-009, Aiming for the Top University and Elite Research Center Development Plan, Center for Nano Science and Technology of National Chiao Tung University, and National Nano Device Laboratories.

1) Y. Li, F. Qian, J. Xiang, and C. M. Lieber: Mater. Today **9** [10] (2006) 18.
2) Y. Huang, X. Duan, Y. Cui, and C. M. Lieber: Nano Lett. **2** (2002) 101.
3) Y. Huang, X. Duan, Y. Cui, L. J. Lauhon, K. H. Kim, and C. M. Lieber: Science **294** (2001) 1313.
4) G. Cheng, A. Kolmakov, Y. Zhang, M. Moskovits, R. Munden, M. A. Reed, G. Wang, D. Moses, and J. Zhang: Appl. Phys. Lett. **83** (2003) 1578.
5) F. Qian, S. Gradeak, Y. Li, C. Y. Wen, and C. M. Lieber: Nano Lett. **5** (2005) 2287.
6) P. G. Collins, M. S. Fuhrer, and A. Zettl: Appl. Phys. Lett. **76** (2000) 894.
7) H. Ouacha, M. Willander, H. Y. Yu, Y. W. Park, M. S. Kabir, H. M. Persson, L. B. Kish, and A. Ouacha: Appl. Phys. Lett. **80** (2002) 1055.
8) S. Reza, Q. T. Huynh, G. Bosman, J. Sippel-Oakley, and A. G. Rinzler: J. Appl. Phys. **99** (2006) 114309.
9) F. Liu, K. L. Wang, D. Zhang, and C. Zhou: Appl. Phys. Lett. **89** (2006) 063116.
10) M. Ishigami, J. H. Chen, E. D. Williams, D. Tobias, Y. F. Chen, and M. S. Fuhrer: Appl. Phys. Lett. **88** (2006) 203116.
11) R. Tarkiainen, L. Roschier, M. Ahlskog, M. Paalanen, and P. Hakonen: Physica E **28** (2005) 57.
12) Y.-M. Lin, J. Appenzeller, J. Knoch, Z. Chen, and P. Avouris: Nano Lett. **6** (2006) 930.
13) H. D. Xiong, W. Wang, Q. Li, C. A. Richter, J. S. Suehle, W.-K. Hong, T. Lee, and D. M. Fleetwood: Appl. Phys. Lett. **91** (2007) 053107.
14) S. L. Rumyantsev, M. S. Shur, M. E. Levinshtein, A. Motayed, and A. V. Davydov: J. Appl. Phys. **103** (2008) 064501.
15) C. Y. Chang, G. C. Chi, W. M. Wang, L. C. Chen, K. H. Chen, F. Ren, and S. J. Pearton: J. Electron. Mater. **35** (2006) 738.
16) C. C. Chen, C. C. Yeh, C. H. Chen, M. Y. Yu, H. L. Liu, J. J. Wu, K. H. Chen, L. C. Chen, J. Y. Peng, and Y. F. Chen: J. Am. Chem. Soc. **123** (2001) 2791.
17) M. J. Buckingham: *Noise Electronic Devices and Systems* (Ellis Horwood, Chichester, U.K., 1983) p. 47.
18) L. C. Li, S. Y. Huang, J. A. Wei, Y. W. Suen, M. W. Lee, W. H. Hsieh, T. W. Liu, and C. C. Chen: J. Nanosci. Nanotechnol. **9** (2009) 1000.
19) H. Nyquist: Phys. Rev. **32** (1928) 110.
20) J. B. Johnson: Phys. Rev. **32** (1928) 97.
21) J. R. Kim, H. So, J. Park, J. Kim, J. Kim, C. J. Lee, and S. C. Lyu: Appl. Phys. Lett. **80** (2002) 3548.
22) T. Kuykendall, P. Pauzauskie, S. Lee, Y. Zhang, J. Goldberger, and P. Yang: Nano Lett. **3** (2003) 1063.
23) L. C. Li, K. H. Huang, Y. W. Suen, W. H. Hsieh, C. D. Chen, M. W. Lee, and C. C. Chen: AIP Conf. Proc. **893** (2007) 731.
24) F. N. Hooge: Phys. Lett. A **29** (1969) 139.
25) L. C. Li, S. Y. Huang, S. F. Jen, S. S. Hong, Y. W. Suen, T. W. Liu, G. M. Hsu, C. C. Chen, L. C. Chen, and K. H. Chen: Proc. 21st Int. Microprocesses and Nanotechnology Conf., 2008, 29D-9-20.